www.lajss.org
Latin American Journal of Solids and Structures 2 (2005) 291–304

Convective heat transfer coefficient for turbulent flow in a porous medium formed by an array of square rods

M.B. Saito and M.J.S. De Lemos*

Laboratório de Computação em Fenômenos de Transporte – LCFT
Departamento de Energia – IEME, Instituto Tecnológico de Aeronáutica – ITA
12228 – 900 – São José dos Campos, SP – Brazil

Abstract

Interfacial convective heat transfer coefficient is calculated for turbulent flow in a porous medium formed by square rods. Such information is needed for turbulent heat transport modeling in porous media when local thermal non-equilibrium is considered. The model considers fluid flowing through a packed bed with arbitrary bed temperature. This adjustment is obtained by solving the microscopic flow governing equations, using high Reynolds formulation and periodic boundary conditions. The numerical methodology employed is based on the control-volume approach with a boundary-fitted non-orthogonal coordinate system. This work intends to obtain functional relationships for the interfacial convective heat transfer coefficient for turbulent low in packed beds.

Keywords: porous media, heat transfer coefficient, thermal non-equilibrium, turbulence model.

1 Introduction

The problem of local thermal non-equilibrium has received considerable attention due to its relevance in a wide variety of engineering applications such as building thermal insulation, nuclear reactor, electronic cooling, multiphase catalytic reactors, etc. The use of two equation model or two energy model is required for these types of problems, which is employed to obtain the temperature difference between the fluid and solid phases. Its use this model has increased in theoretical and numerical research for convection heat transfer processes in porous media.

Kuwahara *et. al* [8] proposed a numerical procedure to determine macroscopic transport coefficients from a theoretical basis without any empiricism. They used a single unit cell and determined the interfacial heat transfer coefficient for the asymptotic case of infinite conductivity of the solid phase. Nakayama et. *al* [10] extended the conduction model of Hsu [7] for treating also convection in porous media. Having established the macroscopic energy equations for

*Corresp. author Email: delemos@ita.br Received 10 October 2005; In revised form 17 October 2005

Notation

A_i	Interface total area between the fluid and solid
c_F	Forchheimer coefficient
c_p	Fluid specific heat
D	Square rods of lateral size
h_i	Interfacial convective heat transfer coefficient
H	Periodic cell height
K	Permeability
k	Turbulence kinetic energy per unit mass
k_f	Fluid thermal conductivity
k_s	Solid thermal conductivity
k	Turbulence kinetic energy per unit mass
P	Pressure
P^*	$P^* = \frac{P-P_{\min}}{P_{\max}-P_{\min}}$, Nondimensional Pressure
Re_D	Reynolds number based on D and the macroscopically uniform velocity
μ	Fluid dynamic viscosity
μ_t	Eddy viscosity
μ_{t_ϕ}	Macroscopic eddy viscosity
ν	Fluid kinematic viscosity
ρ	Fluid density
θ	Dimensionless temperature
ϕ	$\phi = \Delta V_f / \Delta V$, Porosity
φ	General variable
$\langle\varphi\rangle^i$	Intrinsic average
$\langle\varphi\rangle^v$	Volume average
${}^i\varphi$	Spatial deviation

both phases, useful exact solutions were obtained for two fundamental heat transfer processes associated with porous media, namely, steady conduction in a porous slab with internal heat generation within the solid, and also, thermally developing flow through a semi-infinite porous medium.

Saito and de Lemos [18] considered local thermal non-equilibrium and obtained the interfacial heat transfer coefficient for laminar flow using a single unit cell with local instantaneous transport equations.

In all of the above, only laminar flow has been considered. When treating turbulent flow in porous media, however, difficulties arise due to the fact that the flow fluctuates with time and a volumetric average is applied [6]. For handling such situations, a new concept called *double decomposition* has been proposed for developing a macroscopic model for turbulent transport in porous media [12–16]. This methodology has been extended to non-buoyant heat transfer [17],

buoyant flows by [1] and mass transfer by [2]. Based on this same concept, [4] have developed a macroscopic turbulent energy equation for a homogeneous, rigid and saturated porous medium, considering local thermal equilibrium between the fluid and solid matrix. A general classification of all methodologies for treating turbulent flow and heat transfer in porous media has been recently published [3].

This study focuses an turbulent flow through a packed bed where represents an important configuration for efficient heat and mass transfer and suggests the use of equations governing thermal non-equilibrium involving distinct energy balances for both the solid and fluid phases. Accordingly, the use of such two-energy equation model requires an extra parameter to be determined, namely the heat transfer coefficient between the fluid and the solid material [9].

The interfacial heat transfer coefficient for turbulent flow was calculated by [19] using a single unit cell and low Reynolds model. This work proposes a macroscopic heat transfer analysis using a two-energy equation model for conduction and convection mechanisms in porous media. The contribution herein consists in extending the numerical model used in [19] calculating the heat transfer coefficient for turbulent flow considering array high Reynolds.

2 Microscopic transport equations

Microscopic or local time-averaged transport equations for incompressible fluid flow in a rigid homogeneous porous medium have been already presented in the literature and for that they are here just presented (e.g. reference [4]). Furthermore, for turbulent flows the time averaged transport equations can be written as:

$$\text{Continuity: } \nabla \cdot \bar{\mathbf{u}} = 0 \tag{1}$$

$$\text{Momentum: } \rho_f \left[\nabla \cdot (\bar{\mathbf{u}}\,\bar{\mathbf{u}})\right] = -\nabla \bar{p} + \nabla . \left\{ \mu[\nabla \bar{\mathbf{u}} + (\nabla \bar{\mathbf{u}})^T] - \rho \overline{\mathbf{u}'\mathbf{u}'} \right\} \tag{2}$$

where the high Reynolds $k-\varepsilon$ model is used to obtain the eddy viscosity, μ_t, whose equations for the turbulent kinetic energy per unit mass and for its dissipation rate read:

Turbulent kinetic energy per unit mass:

$$\rho_f \left[\nabla \cdot (\bar{\mathbf{u}} k)\right] = \nabla \cdot \left[\left(\mu + \frac{\mu_t}{\sigma_k} \right) \nabla k \right] - \rho \overline{\mathbf{u}'\mathbf{u}'} : \nabla \bar{\mathbf{u}} - \rho \varepsilon \tag{3}$$

Turbulent kinetic energy per unit mass dissipation rate:

$$\rho_f \left[\nabla \cdot (\bar{\mathbf{u}} \varepsilon)\right] = \nabla \cdot \left[\left(\mu + \frac{\mu_t}{\sigma_\varepsilon} \right) \nabla \varepsilon \right] + \left[c_1 \left(-\rho \overline{\mathbf{u}'\mathbf{u}'} : \nabla \bar{\mathbf{u}} \right) - c_2 \rho \varepsilon \right] \frac{\varepsilon}{k} \tag{4}$$

Reynolds stresses and the Eddy viscosity is given by, respectively:

$$-\rho \overline{\mathbf{u}'\mathbf{u}'} = \mu_t \left[\nabla \bar{\mathbf{u}} + (\nabla \bar{\mathbf{u}})^T \right] - \frac{2}{3} \rho k \mathbf{I} \tag{5}$$

$$\mu_t \;=\; \rho\, c_\mu\, \frac{k^2}{\varepsilon} \tag{6}$$

where, ρ is the fluid density, p is the pressure, μ represents the fluid viscosity.

In the above equation setσ_k, σ_ε, c_1, c_2, and c_μ are dimensionless constants given as follows,

$$c_\mu = 0.09, \quad c_1 = 1.44, \quad c_2 = 1.92, \quad \sigma_k = 1.0, \quad \sigma_\varepsilon = 1.3.$$

Also, the time averaged energy equations become:

$$\text{Energy - Fluid Phase: } (\rho c_p)_f \left\{ \nabla \cdot \left(\bar{\mathbf{u}} \bar{T}_f \right) \right\} = \nabla \cdot \left(k_f \nabla \bar{T}_f \right) - (\rho c_p)_f \nabla \cdot \left(\overline{\mathbf{u}' T_f'} \right) + S_f \tag{7}$$

$$\text{Energy - Solid Phase (Porous Matrix): } \nabla \cdot \left(k_s \nabla \bar{T}_s \right) + S_s = 0 \tag{8}$$

where the subscripts f and s refer to fluid and solid phases, respectively. Here, T is the temperature, k_f is the fluid thermal conductivity, k_s is the solid thermal conductivity, c_p is the specific heat and S is the heat generation term. If there is no heat generation either in the solid or in the fluid, one has further$S_f \;=\; S_s \;=\; 0$.

3 Decomposition of flow variables in space and time

Macroscopic transport equations for turbulent flow in a porous medium are obtained through the simultaneous application of time and volume average operators over a generic fluid property φ [6]. Such concepts are mathematically defined as,

$$\bar{\varphi} = \frac{1}{\Delta t} \int_t^{t+\Delta t} \varphi \; dt, \quad \text{with} \quad \varphi = \bar{\varphi} + \varphi' \tag{9}$$

$$\langle \varphi \rangle^i = \frac{1}{\Delta V_f} \int\limits_{\Delta V_f} \varphi \, dV; \;\; \langle \varphi \rangle^v = \phi \langle \varphi \rangle^i; \;\; \phi = \frac{\Delta V_f}{\Delta V}, \quad \text{with} \quad \varphi = \langle \varphi \rangle^i + {}^i\varphi \tag{10}$$

where ΔV_f is the volume of the fluid contained in a Representative Elementary Volume (REV) ΔV, intrinsic average and volume average are represented, respectively, by $\langle \; \rangle^i$ and $\langle \; \rangle^v$. Also, the left superscript i represents spatial deviation.

The *double decomposition* idea introduced and fully described in [12–16], combines Eqs. (9)-(10) and can be summarized as:

$$\overline{\langle \varphi \rangle^i} \;=\; \langle \bar{\varphi} \rangle^i; \quad {}^i\bar{\varphi} \;=\; \overline{{}^i\varphi}; \quad \langle \varphi' \rangle^i \;=\; \langle \varphi \rangle^{i'} \tag{11}$$

and,

$$\left.\begin{array}{l} \varphi' \;=\; \langle \varphi' \rangle^i + {}^i\varphi' \\ {}^i\varphi \;=\; \overline{{}^i\varphi} + {}^i\varphi' \end{array}\right\} \quad \text{where} \quad {}^i\varphi' \;=\; \varphi' - \langle \varphi' \rangle^i \;=\; {}^i\varphi - \overline{{}^i\varphi} \tag{12}$$

Therefore, the quantity φ can be expressed by either,

$$\varphi = \overline{\langle\varphi\rangle^i} + \langle\varphi\rangle^{i'} + \overline{{}^i\varphi} + {}^i\varphi', \tag{13}$$

or

$$\varphi = \langle\bar{\varphi}\rangle^i + {}^i\bar{\varphi} + \langle\varphi'\rangle^i + {}^i\varphi'. \tag{14}$$

The term ${}^i\varphi'$ can be viewed as either the temporal fluctuation of the spatial deviation or the spatial deviation of the temporal fluctuation of the quantityφ.

4 Macroscopic flow and energy equations

When the average operators (9)-(10) are simultaneously applied over Eqs. (1)-(2), macroscopic equations for turbulent flow are obtained. Volume integration is performed over a Representative Elementary Volume (REV) [6], [20], resulting in,

$$\text{Continuity: } \nabla\cdot\bar{\mathbf{u}}_D = 0 \tag{15}$$

where, $\bar{\mathbf{u}}_D = \phi\langle\bar{\mathbf{u}}\rangle^i$ and $\langle\bar{\mathbf{u}}\rangle^i$ identifies the intrinsic (liquid) average of the time-averaged velocity vector $\bar{\mathbf{u}}$.

Momentum:

$$\begin{array}{l}\rho\left[\frac{\partial\bar{\mathbf{u}}_D}{\partial t} + \nabla\cdot\left(\frac{\bar{\mathbf{u}}_D\bar{\mathbf{u}}_D}{\phi}\right)\right] = -\nabla(\phi\langle\bar{p}\rangle^i) + \mu\nabla^2\bar{\mathbf{u}}_D - \nabla\cdot(\rho\phi\langle\overline{\mathbf{u}'\mathbf{u}'}\rangle^i) \\ \quad - \left[\frac{\mu\phi}{K}\bar{\mathbf{u}}_D + \frac{c_F\phi\rho|\bar{\mathbf{u}}_D|\bar{\mathbf{u}}_D}{\sqrt{K}}\right]\end{array}, \tag{16}$$

where the last two terms in Eq. (16) represent the Darcy and Forchheimer contributions by [5]. The symbol K is the porous medium permeability, c_F is the form drag or Forchheimer coefficient, $\langle\bar{p}\rangle^i$ is the intrinsic average pressure of the fluid and ϕ is the porosity of the porous medium.

The macroscopic Reynolds stress, $-\rho\phi\langle\overline{\mathbf{u}'\mathbf{u}'}\rangle^i$, appearing in Eq. (16) is given as,

$$-\rho\phi\langle\overline{\mathbf{u}'\mathbf{u}'}\rangle^i = \mu_{t_\phi}2\langle\bar{\mathbf{D}}\rangle^{\mathbf{v}} - \frac{2}{3}\phi\rho\langle k\rangle^i\mathbf{I}, \tag{17}$$

where,

$$\langle\bar{\mathbf{D}}\rangle^v = \frac{1}{2}\left[\nabla(\phi\langle\bar{\mathbf{u}}\rangle^i) + [\nabla(\phi\langle\bar{\mathbf{u}}\rangle^i)]^T\right], \tag{18}$$

is the macroscopic deformation tensor, $\langle k\rangle^i = \langle\overline{\mathbf{u}'\cdot\mathbf{u}'}\rangle^i/2$ is the intrinsic turbulent kinetic energy, and μ_{t_ϕ}, is the turbulent viscosity, which is modeled in [3] similarly to the case of clear flow, in the form,

$$\mu_{t_\phi} = \rho c_\mu\frac{\langle k\rangle^{i^2}}{\langle\varepsilon\rangle^i}, \tag{19}$$

The intrinsic turbulent kinetic energy per unit mass and its dissipation rate are governed by the following equations,

$$\begin{array}{l}\rho\left[\frac{\partial}{\partial t}\left(\phi\langle k\rangle^i\right)+\nabla\cdot\left(\bar{\mathbf{u}}_D\langle k\rangle^i\right)\right]=\nabla\cdot\left[\left(\mu+\frac{\mu_{t_\phi}}{\sigma_k}\right)\nabla\left(\phi\langle k\rangle^i\right)\right]-\rho\langle\overline{\mathbf{u}'\mathbf{u}'}\rangle^i:\nabla\bar{\mathbf{u}}_D \\ +c_k\rho\frac{\phi\langle k\rangle^i|\bar{\mathbf{u}}_D|}{\sqrt{K}}-\rho\phi\langle\varepsilon\rangle^i\end{array} . \quad (20)$$

$$\begin{array}{l}\rho\left[\frac{\partial}{\partial t}\left(\phi\langle\varepsilon\rangle^i\right)+\nabla\cdot\left(\bar{\mathbf{u}}_D\langle\varepsilon\rangle^i\right)\right]=\nabla\cdot\left[\left(\mu+\frac{\mu_{t_\phi}}{\sigma_\varepsilon}\right)\nabla\left(\phi\langle\varepsilon\rangle^i\right)\right]+c_1\left(-\rho\langle\overline{\mathbf{u}'\mathbf{u}'}\rangle^i:\nabla\bar{\mathbf{u}}_D\right)\frac{\langle\varepsilon\rangle^i}{\langle k\rangle^i} \\ +c_2\,c_k\rho\frac{\phi\langle\varepsilon\rangle^i|\bar{\mathbf{u}}_D|}{\sqrt{K}}-c_2\,\rho\phi\frac{\langle\varepsilon\rangle^{i^2}}{\langle k\rangle^i}\end{array} . \quad (21)$$

where, c_k, c_1, c_2 and c_μ are nondimensional constants.

Similarly, macroscopic energy equations are obtained for both fluid and solid phases by applying time and volume average operators to Eqs. (7) and (8). As in the flow case, volume integration is performed over a Representative Elementary Volume (REV), resulting in,

$$\begin{array}{l}(\rho\,c_p)_f\left[\frac{\partial\,\phi\langle\overline{T_f}\rangle^i}{\partial\,t}+\nabla\cdot\left\{\phi\left(\langle\bar{\mathbf{u}}\rangle^i\langle\overline{T_f}\rangle^i+\langle{}^i\bar{\mathbf{u}}^i\overline{T_f}\rangle^i+\langle\overline{\mathbf{u}'\,T_f'}\rangle^i\right)\right\}\right]=\nabla\cdot\left[k_f\nabla\left(\phi\,\langle\overline{T_f}\rangle^i\right)\right] \\ +\nabla\cdot\left[\frac{1}{\Delta V}\int\limits_{A_i}\mathbf{n}_i\,k_f\overline{T_f}\,dA\right] \\ +\frac{1}{\Delta V}\int\limits_{A_i}\mathbf{n}_i\cdot k_f\nabla\overline{T_f}\,dA\end{array} , \quad (22)$$

$$\begin{array}{l}(\rho\,c_p)_s\left\{\frac{\partial\,(1-\phi)\,\langle\overline{T_s}\rangle^i}{\partial\,t}\right\}=\nabla\cdot\left\{k_s\nabla\left[(1-\phi)\,\langle\overline{T_s}\rangle^i\right]\right\}-\nabla\cdot\left[\frac{1}{\Delta V}\int\limits_{A_i}\mathbf{n}_i\,k_s\overline{T_s}\,dA\right] \\ -\frac{1}{\Delta V}\int\limits_{A_i}\mathbf{n}_i\cdot k_s\nabla\overline{T_s}\,dA\end{array} , \quad (23)$$

where $\langle\overline{T_s}\rangle^i$ and $\langle\overline{T_f}\rangle^i$ denote the intrinsic average temperature of solid and fluid phases, respectively, A_i is the interfacial area within the REV and $\mathbf{n}_i$ is the unit vector normal to the fluid-solid interface, pointing from the fluid towards the solid phase. Eqs. (22) and (23) are the macroscopic energy equations for the fluid and the porous matrix (solid), respectively.

Further, using the *double decomposition concept* given by Eq. (11)-(14), Rocamora and de Lemos [17] have shown that the fourth term on the left hand side of Eq. (22) can be expressed as:

$$\langle\overline{\mathbf{u}'T_f'}\rangle^i=\langle\overline{(\langle\mathbf{u}'\rangle^i+{}^i\mathbf{u}')\,(\langle T_f'\rangle^i+{}^iT')}\rangle^i=\overline{\langle\mathbf{u}'\rangle^i\langle T_f'\rangle^i}+\langle\overline{{}^i\mathbf{u}'\,{}^iT_f'}\rangle^i. \quad (24)$$

Therefore, in view of Eq. (24), Eq. (22) can be rewritten as:

$$\begin{array}{l}(\rho\,c_p)_f\left[\frac{\partial\,\phi\langle\overline{T_f}\rangle^i}{\partial\,t}+\nabla\cdot\left\{\phi\left(\langle\bar{\mathbf{u}}\rangle^i\langle\overline{T_f}\rangle^i+\langle{}^i\bar{\mathbf{u}}^i\overline{T_f}\rangle^i+\overline{\langle\mathbf{u}'\rangle^i\langle T_f'\rangle^i}+\langle\overline{{}^i\mathbf{u}'\,{}^iT_f'}\rangle^i\right)\right\}\right]= \\ \nabla\cdot\left[k_f\nabla\left(\phi\,\langle\overline{T_f}\rangle^i\right)\right]+\nabla\cdot\left[\frac{1}{\Delta V}\int\limits_{A_i}\mathbf{n}_i\,k_f\overline{T_f}\,dA\right]+\frac{1}{\Delta V}\int\limits_{A_i}\mathbf{n}_i\cdot k_f\nabla\overline{T_f}\,dA\end{array} . \quad (25)$$

5 Interfacial heat transfer coefficient

In Eqs. (23) and (25) the heat transferred between the two phases can be modeled by means of a film coefficient h_i such that,

$$h_i a_i \left(\langle \overline{T_s} \rangle^i - \langle \overline{T_f} \rangle^i \right) = \frac{1}{\Delta V} \int\limits_{A_i} \mathbf{n}_i \cdot k_f \nabla \overline{T_f} \, dA = \frac{1}{\Delta V} \int\limits_{A_i} \mathbf{n}_i \cdot k_s \nabla \overline{T_s} \, dA. \tag{26}$$

where, h_i is known as the interfacial convective heat transfer coefficient and $a_i = A_i/\Delta V$ is the surface area per unit volume.

For determiningh_i, Kuwahara *et. al* [8] modeled a porous medium by considering an infinite number of solid square rods of size D, arranged in a regular triangular pattern (see Fig. 1). They numerically solved the governing equations in the void region, exploiting to advantage the fact that for an infinite and geometrically ordered medium a repetitive cell can be identified. Periodic boundary conditions were then applied for obtaining the temperature distribution under fully developed flow conditions. A numerical correlation for the interfacial convective heat transfer coefficient was proposed by Kuwahara *et. al* [8] for laminar flow as,

$$\frac{h_i D}{k_f} = \left(1 + \frac{4(1-\phi)}{\phi} \right) + \frac{1}{2}(1-\phi)^{1/2} Re_D \overset{1/3}{\mathrm{Pr}}, \qquad \text{valid for} \quad 0.2 < \phi < 0.9 \tag{27}$$

Eq. (27) is based on porosity dependency and is valid for packed beds of particle diameter$D$.

Saito and de Lemos [18] obtained the interfacial heat transfer coefficient for laminar flows though an infinite square rod; this same physical model will be used here for obtaining the interfacial heat transfer coefficient h_i for turbulent flows.

6 Periodic cell and boundary conditions

In order to evaluate the numerical tool to be used in the determination of the film coefficient given by Eq. (26), a test case was run for obtaining the flow field in a periodic cell, which is here assumed to represent the porous medium. Consider a macroscopically uniform flow through an infinite number of square rods of lateral size D, placed in a staggered arrangement and maintained at constant temperature T_w. The periodic cell or representative elementary volume, ΔV, is schematically showed in Fig. 1 and has dimensions $2H \times H$. Computations within this cell were carried out using a non-uniform grid, as shown in Fig. 2, to ensure that the results were grid independent. The Reynolds number $Re_D = \rho \, \bar{\mathbf{u}}_D D/\mu$ was varied from 10^4 to 10^6 and the porosity,$\phi = 1 - (D/H)^2$.

The numerical method utilized to discretize the flow and energy equations in the unit cell is the Control Volume approach. The SIMPLE method of Patankar [11] was used for handling Eq. (1)-(8) the velocity-pressure coupling. Convergence was monitored in terms of the normalized

residue for each variable. The maximum residue allowed for convergence check was set to 10^{-9}, being the variables normalized by appropriate reference values.

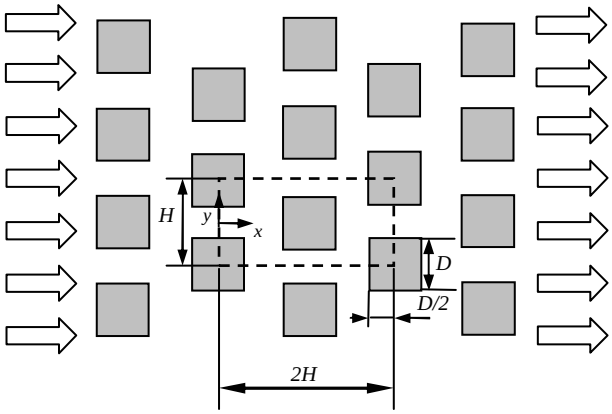

Figure 1: Physical model and coordinate system.

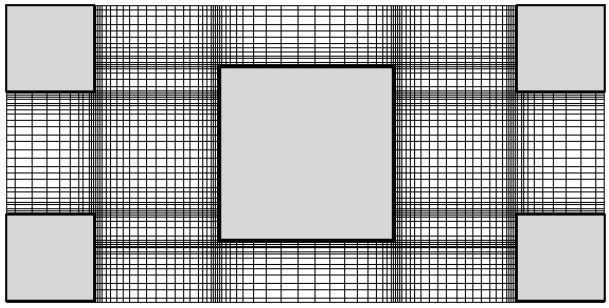

Figure 2: Non uniform computational grid.

For fully developed flow in the cell of Fig. 1, the velocity at exit ($x/H = 2$) must be identical to that at the inlet ($x/H = 0$). Temperature profiles, however, are only identical at both cell exit and inlet if presented in terms of an appropriate non-dimensional variable. The situation is analogous to the case of forced convection in a channel with isothermal walls; see [19]. Thus, boundary conditions and periodic constraints are given by:

On the solid walls:

$$\frac{\bar{u}}{u_\tau} = \frac{1}{\kappa}\ln\left(n^+\mathrm{E}\right), \quad k = \frac{u_\tau^2}{c_\mu^{1/2}}, \quad \varepsilon = \frac{c_\mu^{3/4} k_w^{3/2}}{\kappa\, n_w}, \quad q_w = \frac{\left(\rho\, c_p\right)_f C_\mu^{1/4} k_w^{1/2} \left(\bar{T} - T_w\right)}{\left(\frac{\mathrm{Pr}_t}{\kappa}\ln\left(n_w^+\right) + C_Q\left(\mathrm{Pr}\right)\right)} \tag{28}$$

where, $u_\tau = \left(\frac{\tau_w}{\rho}\right)^{1/2}$, $n_w^+ = \frac{n_w\, u_\tau}{\nu}$, $C_Q = 12.5\ \mathrm{Pr}^{2/3} + 2.12\ln\left(\mathrm{Pr}\right) - 5.3$ for $\mathrm{Pr} > 0.5$
where, Pr and Pr_t are Prandtl and turbulent Prandtl number, respectively, q_w is wall heat flux,

u_τ is wall-friction velocity, n_w is the coordinate normal to wall, κ is constant for turbulent flow past smooth impermeable walls or von Kármán's constant and E is an integration constant that depends on the roughness of the wall. For smooth walls with constant shear stress E = 9.

On the symmetry planes:

$$\frac{\partial \bar{u}}{\partial y} = \frac{\partial \bar{v}}{\partial y} = \frac{\partial k}{\partial y} = \frac{\partial \varepsilon}{\partial y} = 0, \tag{29}$$

where $\bar{u}$ and $\bar{v}$ are components of $\bar{\mathbf{u}}$.

On the periodic boundaries:

$$\bar{u}|_{inlet} = \bar{u}|_{outlet}, \quad \bar{v}|_{inlet} = \bar{v}|_{outlet}, \quad k|_{inlet} = k|_{outlet}, \quad \varepsilon|_{inlet} = \varepsilon|_{outlet}, \tag{30}$$

$$\theta\,|_{inlet} = \theta\,|_{outlet} \Leftrightarrow \left.\frac{\bar{T} - \bar{T}_w}{\bar{T}_B(x) - \bar{T}_w}\right|_{inlet} = \left.\frac{\bar{T} - \bar{T}_w}{\bar{T}_B(x) - \bar{T}_w}\right|_{outlet}, \tag{31}$$

The bulk mean temperature of the fluid is given by:

$$\bar{T}_B(x) = \frac{\int \bar{u}\bar{T}dy}{\int \bar{u}dy} \tag{32}$$

Computations are based on the Darcy velocity, the length of structural unit H and the temperature difference$\left(\bar{T}_B(x) - \bar{T}_w\right)$, as references scales.

6.1 Film coefficient h_i

Determination of h_i is here obtained by calculating, for the unit cell of Fig. 1, an expression given as,

$$h_i = \frac{Q_{total}}{A_i\,\Delta T_{ml}} \tag{33}$$

where $A_i = 8D \quad \times 1$. The overall heat transferred in the cell, Q_{total}, is giving by,

$$Q_{total} = (H - D)\rho\,\bar{u}_B\,c_p\,\left(\bar{T}_B\big|_{outlet} - \bar{T}_B\big|_{inlet}\right), \tag{34}$$

The bulk mean velocity of the fluid is given by:

$$\bar{u}_B(x) = \frac{\int \bar{u}dy}{\int dy} \tag{35}$$

and the logarithm mean temperature difference, ΔT_{ml} is,

$$\Delta T_{ml} = \frac{\left(\bar{T}_w - \bar{T}_B\big|_{outlet}\right) - \left(\bar{T}_w - \bar{T}_B\big|_{inlet}\right)}{\ln\left[(\bar{T}_w - \bar{T}_B\big|_{outlet})(\bar{T}_w - \bar{T}_B\big|_{inlet})\right]} \tag{36}$$

Eq. 34 represents an overall heat balance on the entire cell and associates the heat transferred to the fluid to a suitable temperature differenceΔT_{ml}. As mentioned earlier, Eqs. 1-8 were numerically solved in the unit cell until conditions Eqs. 30-31 were satisfied.

7 Results and discussion

7.1 Periodic flow

Results for velocity and temperature fields were obtained for different Reynolds numbers. In order to assure that the flow is hydrodynamically and thermally developed in the periodic cell of Fig. 1, the governing equations were solved repetitively in the cell, taking the outlet profiles for $\bar{\mathbf{u}}$ and θ at exit and plugging them back at inlet. In the first run, uniform velocity and temperature profiles were set at the cell entrance for Pr = 1 and $Re_D = 10^5$, giving θ=1 at x/H=0. Then, after convergence of the flow and temperature fields, $\bar{\mathbf{u}}$ and θ at x/H=2 were used as inlet profiles for a second run, corresponding to solving again the flow for a similar cell beginning in x/H=2. Similarly, a third run was carried out and again outlet results, this time corresponding to an axial position x/H=4, were recorded. This procedure was repeated several times until $\bar{\mathbf{u}}$ and θ did not differ substantially at both inlet and outlet positions. Resulting non-dimensional velocity and temperature profiles are shown in Fig. 3 and Fig. 4, respectively, showing that the periodicity constraints imposed by Eqs. 30-31 was satisfied for $x/H > 4$. For the entrance region ($0 < x/H < 4$), θ profiles change with length x/H being essentially invariable after this distance. Under this condition of constant θ profile, the flow was considered to be macroscopically developed for Re_D up to 10^6.

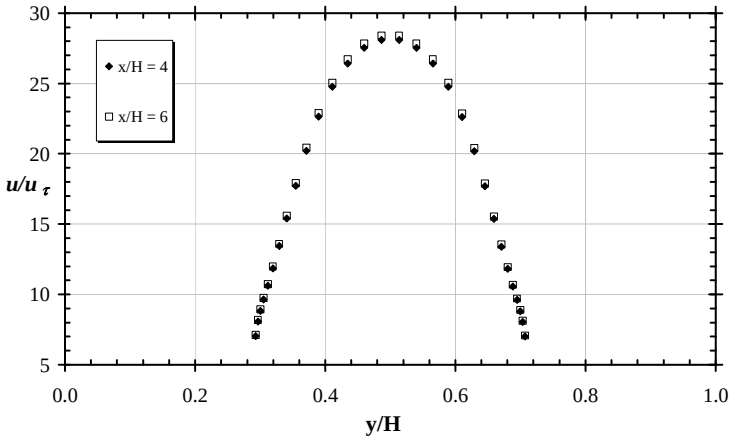

Figure 3: Dimensionless velocity profile for Pr = 1 and $Re_D = 10^5$.

7.2 Developed flow and temperature fields

Macroscopically developed flow field for $Pr = 1$ and $Re_D = 10^5$ is presented in Fig. 5, corresponding to x/D=6 at the cell inlet. The flow accelerates when forced in between the gap formed by two rods, separating past the rod edges and impinging against the rod left faces. The expression "macroscopically developed" is used herein to account for the fact that periodic flow

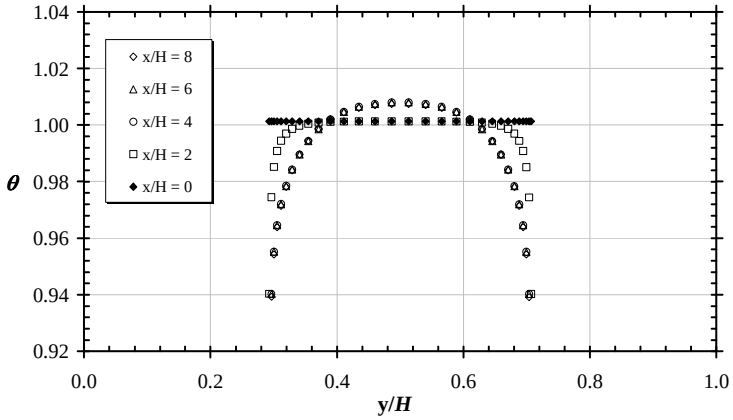

Figure 4: Dimensionless temperature profile for Pr = 1 and $Re_D = 10^5$.

has been achieved at that axial position. Fig. 6 presents levels of turbulence kinetic energy, which are higher around the rod corners where a strong shear layer is formed. Further downstream the rods in the weak region, steep velocity gradients appear due to flow deceleration, also increasing there the local level of k. Temperature distribution is shown in Fig. 7, also for Re_D=10^5. Colder fluid impinges on the rod left side yielding strong temperature gradients on that face. Downstream the obstacles, fluid recirculation smoothes temperature gradients and deforms isotherms within the mixing region. When the Reynolds number is sufficiently high (not shown here), thermal boundary layers cover the rod surfaces indicating that convective heat transfer overwhelms thermal diffusion.

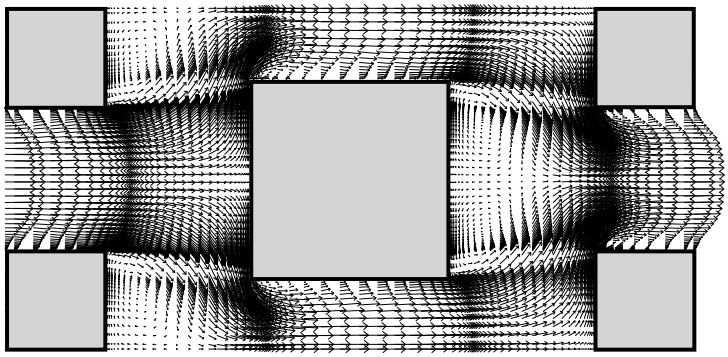

Figure 5: Velocity field for $Re_D = 10^5$, $\phi = 0.65$ and $6 < x/H < 8$

Once fully developed flow and temperature fields are achieved, for the fully developed condition ($x > 6H$), bulk temperatures were calculated according to Eq. 32, at both inlet and outlet positions. They were then used to calculate h_i using Eqs. 33-36. Results for h_i are plotted in Fig. 8 for Re_D up to 10^6. Also plotted in this figure are results computed with correlation (27)

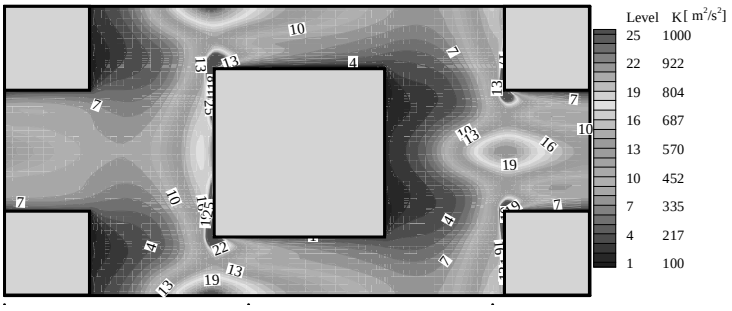

Figure 6: Turbulence kinetic energy for $Re_D = 10^5$ and ϕ=0.65.

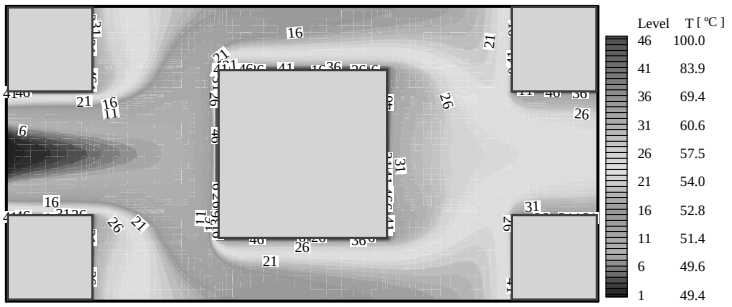

Figure 7: Isotherms for Pr = 1, $Re_D = 10^5$ and $\phi = 0.65$

using $\phi = 0.65$. The figure seems to indicate that both computations show a reasonable agreement for laminar results. The numerical correlation for the interfacial convective heat transfer coefficient was proposed by Kuwahara *et. al* [8] is used only for laminar flows while for turbulent results a correlation is needed that is the long term objective of the present research endeavour and results herein represent the first step towards such goal.

8 Concluding remarks

A computational procedure for determining the convective coefficient of heat exchange between the porous substrate and the working fluid for a porous medium was detailed. As a preliminary result, a macroscopically uniform laminar and turbulent flow through a periodic cell of isothermal square rods was computed, considering periodical velocity and temperature fields. Quantitative agreement was obtained when comparing the preliminary laminar results herein with simulations by Kuwahara *et. al* [8]. Saito and de Lemos [19] and this work obtained the heat transfer coefficient for turbulent flow using low and high Reynolds, respectively, by mean a single unit cell formed by an array of square rods. Moreover, the numerical correlation for the interfacial convective heat transfer coefficient for turbulent flow is needed. Further work will be carried

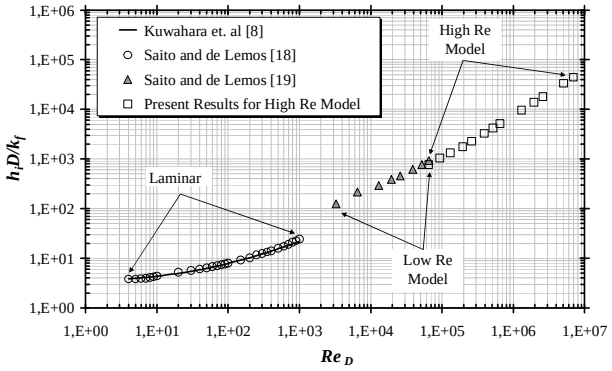

Figure 8: Effect of Re_D on h_i for $Pr = 1$ with correlation of Kuwahara *et. al* [8].

out in order to simulate fully turbulent flow and heat transfer in a porous medium formed by an array of elliptic, cylindrical and transverse elliptic rods. Ultimately, it is expected that a correlation for the heat transfer coefficient be obtained so that the exchange energy between the solid and the fluid can be accounted for.

Acknowledgements: The authors are grateful to CNPq and FAPESP, Brazil, for their invaluable support during the preparation of this work.

References

[1] M.J.S. de Lemos and E.J. Braga. Modeling of turbulent natural convection in porous media. *International Communications in Heat and Mass Transfer*, 30(5):615–624, 2003.

[2] M.J.S. de Lemos and M.S. Mesquita. Turbulent mass transport in saturated rigid porous media. *International Communications in Heat and Mass Transfer*, 30(1):105–115, 2003.

[3] M.J.S. de Lemos and M.H.J. Pedras. Recent mathematical models for turbulent flow in saturated rigid porous media. *Journal of Fluids Engineering*, 123(4):935–940, 2001.

[4] M.J.S. de Lemos and F.D. Rocamora Jr. Turbulent transport modeling for heated flow in rigid porous media. In *Proc. of IHTC12 - 12th International Heat Transfer Conference*, Grenoble, França, 18-23 August, 2002.

[5] P. Forchheimer. *Wasserbewegung durch Boden*, volume 45. Z. Ver. Deutsch. Ing., 1901.

[6] W.G. Gray and P. C. Y. Lee. On the theorems for local volume averaging of multiphase system. *Int. J. Multiphase Flow*, 3:333–340, 1977.

[7] C.T. Hsu. A closure model for transient heat conduction in porous media. *Journal of Heat Transfer*, 121:733–739, 1999.

[8] F. Kuwahara, M. Shirota, and A. Nakayama. A numerical study of interfacial convective heat transfer coefficient in two-energy equation model for convection in porous media. *Int. J. Heat Mass Transfer*, 44:1153–1159, 2001.

[9] A.V. Kuznetsov. *Thermal Nonequilibrium Forced Convection in Porous Media*. Elsevier Sc., Oxford, 1998.

[10] A. Nakayama, F. Kuwahara, M. Sugiyama, and G. Xu. A two-energy equation model for conduction and convection in porous media. *Int. J. Heat Mass Transfer*, 44:4375–4379, 2001.

[11] S.V. Patankar. *Numerical Heat Transfer and Fluid Flow*. Mc-Graw Hill, 1980.

[12] M.H.J. Pedras and M.J.S. de Lemos. On the definition of turbulent kinetic energy for flow in porous media. *International Communications in Heat and Mass Transfer*, 27(2):211–220, 2000.

[13] M.H.J. Pedras and M.J.S. de Lemos. Macroscopic turbulence modeling for incompressible flow through undeformable porous media. *International Journal of Heat and Mass Transfer*, 44(6):1081–1093, 2001a.

[14] M.H.J. Pedras and M.J.S. de Lemos. Simulation of turbulent flow in porous media using a spatially periodic array and a lowre two-equation closure. *Numerical Heat Transfer Part A – Applications*, 39(1), 2001b.

[15] M.H.J. Pedras and M.J.S. de Lemos. On the mathematical description and simulation of turbulent flow in a porous medium formed by an array of elliptic rods. *Journal of Fluids Engineering*, 123(4):941–947, 2001c.

[16] M.H.J. Pedras and M.J.S. de Lemos. Computation of turbulent flow in porous media using a low reynolds $k-\varepsilon$ model and an infinite array of transversally-displaced elliptic rods. *Numerical Heat Transfer Part A – Applications*, 43(6):585–602, 2003.

[17] F.D. Rocamora Jr and M.J.S. de Lemos. Analysis of convective heat transfer for turbulent flow in saturated porous media. *International Communications in Heat and Mass Transfer*, 27(6):825–834, 2000.

[18] M.B. Saito and M.J.S. de Lemos. Interfacial heat transfer coefficient for non-equilibrium convective transport in porous media. *International Communications in Heat and Mass Transfer*, 32:667–677, 2004a.

[19] M.B. Saito and M.J.S. de Lemos. Turbulent heat transfer coefficient in an infinite array of square rods simulated with a low-reynolds $k-\varepsilon$ model. In *Proc. of ETT2004 IV Escola Brasileira de Primavera de Transição e Turbulência*, Porto Alegre, RS, Brasil, 2004b.

[20] J.C. Slattery. Flow of viscoelastic fluids through porous media. *A.I.Ch.E. J.*, 13:1066–1071, 1967.